

Accepted for Publication ApJ Main Journal Nov 2002

Azimuthal and Kinematic Segregation of Neutral and Molecular Gas in Arp 118: The Yin-Yang Galaxy NGC 1144

P. N. Appleton

SIRTF Science Center, MS 220-6, California Institute of Technology, Pasadena CA 91125

apple@ipac.caltech.edu

V. Charmandaris

Astronomy Department, Cornell University, 106 Space Sciences Bldg, Ithaca NY 14853

vassilis@astro.cornell.edu

Yu Gao

*IPAC, MS 100-22, Infrared Processing & Analysis Center, Caltech, Pasadena CA 91125 &
Department of Astronomy, University of Massachusetts, LGRT-B 619E, 710 North
Pleasant Street, Amherst, MA 01003-9305*

gao@ipac.caltech.edu

Tom Jarrett

IPAC, MS 100-22, Infrared Processing & Analysis Center, Caltech, Pasadena CA 91125

jarrett@ipac.caltech.edu

M. A. Bransford

IBM, 3605 Hwy 52 North, Rochester, MN 55901

bransma@us.ibm.com

ABSTRACT

We present new high-resolution HI observations of the disk of the collisional infrared luminous ($L_{\text{IR}} = 2.2 \times 10^{11} L_{\odot}$) galaxy NGC 1144, which reveal an apparent large-scale azimuthal and kinematic segregation of neutral hydrogen relative

to the molecular gas distribution. Even among violently collisional galaxies, the CO/HI asymmetry in NGC 1144 is unusual, both in the inner regions, and in the outer disk. We suggest that we are observing Arp 118 at a special moment, shortly after a high-speed collision between NGC 1144 and its elliptical companion NGC 1143. HI emission with an average molecular fraction $f_{mol} < 0.5$ is observed on one side (NW) of the rotating disk of NGC 1144, while the other side (SE) is dominated by dense molecular complexes in which f_{mol} is almost unity. The interface region between the warm- and cool-cloud dominated regions, lies on a deep spiral-like dust-lane which we identify as a shock-wave responsible for the relative shift in the dominance of HI and H₂ gas. A strong shock being fed by diffuse HI clouds with unusually large ($> 400 \text{ km s}^{-1}$) rotational velocities can explain: 1) the CO/HI asymmetries, 2) a large velocity jump (185 km s^{-1}) across the arm as measured by HI absorption against a radio bright continuum source which straddles the arm, and 3) the asymmetric distribution of star formation and off-nuclear molecular gas resulting from likely streaming motions associated with the strong-shock. The new results provide for the first time a coherent picture of Arp 118’s many peculiarities, and underlines the potentially complex changes in the gas-phase that can accompany large gravitational perturbations of gas-rich galaxies.

Subject headings: infrared: galaxies — galaxies: individual (NGC 1143, NGC 1144) — galaxies: interactions (Arp 118) — galaxies: Seyfert — galaxies: starburst

1. Introduction

It is now well known that galaxies in an intermediate stage of merger conspire to create high concentrations of molecules in their nuclear regions (Sargent & Scoville 1991; Scoville et al. 1991; Sanders & Mirabel 1996; Bryant & Scoville 1999). The creation of these centrally concentrated molecular reservoirs may be quite rapid because cases are rare in which molecular gas has not yet settled to the center—although some are known (Lo, Gao & Gruendl 1997; Casoli et al. 1999; Yun & Hibbard 2001; Wang et al. 2001; Appleton et al. 2002). In a small subset of cases, only one of the two participating galaxies contains nuclear CO (Dinh-V-Trung et al. 2001; Evans et al. 2002), suggesting that the process of central gas accumulation is complex—perhaps depending on the details of the collision geometry, the initial gas content of the participants, or other special circumstances (Chen et al. 2002; Yun & Hibbard 2001).

There is little detailed knowledge of the effects of galaxy collisions/mergers on the

molecular fraction, $f_{mol} = M_{mol}/(M_{mol} + M_{HI})$, of the participating host galaxy disks. The fate of any pre-existing neutral hydrogen in the disk of a collisional galaxy might be expected to follow two different paths in major merger. HI in the outer galaxy is likely to become incorporated into tidal tails, where it might survive the merger-at least temporarily (Hibbard & van Gorkom 1996; Mihos 2001). On the other hand, HI and pre-existing molecular material in the inner galaxy is more likely to become involved in inflows (Noguchi 1988; Bekki & Noguchi 1994; Barnes & Hernquist 1996; Mihos & Hernquist 1996). Hibbard et al. (1994) speculated that the deficiency of HI in the inner regions of NGC 7252 was a direct result of it being converted into other forms (ionized gas, stars) through shock heating, a process that might lead to an apparent segregation of molecular and HI gas in merging systems in general (e.g. Duc et al. 1997; Braine et al. 2001; Yun & Hibbard 2001). The high concentrations of molecular gas in the nuclei of Luminous Infrared Galaxies (LIRGs) and Ultra-luminous Infrared Galaxies (ULIRGs) (Sanders & Mirabel 1996) could be taken as evidence that some of the pre-existing HI is converted into molecular form, but such ideas must be qualified by the fact that most estimates of the molecular gas mass depend on a highly uncertain conversion factor from the CO line flux to molecular hydrogen column density (e.g. Sanders & Mirabel 1985; Scoville et al. 1989; Downes & Solomon 1998; Bryant & Scoville 1999).

Whatever the final outcome of any pre-existing gas in a merger, it is likely that at least some of it will undergo a change of phase during a violent encounter (Gao & Solomon 1999; Georgakakis, Forbes & Norris 2000), especially if it experiences compression, or enters a high-pressure starburst region. Various models governing such transformations have been outlined by Jog & Solomon (1992) specifically for starburst nuclei, and by Elmegreen (1993) for a more general ISM environment.

In this paper we demonstrate that HI/CO segregation (defined here as a separation of two regions with vastly different molecular fractions) can occur outside the context of tidal bridges and tails: in this case *within the rotating disk* of a violently interacting galaxy with regular (albeit rapid) rotation. We present new high resolution 21cm HI observations of the interacting galaxy pair Arp 118, comprising of the disk galaxy NGC 1144, and the elliptical/S0 companion NGC 1143 (see Table 1). An optical image of the system is presented in Figure 1. It is believed that NGC 1143 has reached its current position on the sky after having collided with NGC 1144 – moving on a north-westerly path (Lamb, Hearn & Gao 1998). NGC 1144 has been classified as a ring galaxy by Freeman & de Vaucouleurs (1974), but its actual morphology is far from simple (see Joy & Ghigo 1988). Despite the identification of peculiar arc-segments and ring-like structures (Hippelein 1989), the H α velocity field shows remarkable regularity (see Bransford et al. 1999, – hereafter B99) suggesting that it rotates in a counter-clockwise manner as projected onto the sky. The most dramatic feature of its optical disk is a very extensive dark dust-lane which originates east of the nucleus and

extends outwards curving to the north and west (see B99). If this is a trailing feature, then the plane of the disk of NGC 1144 is tilted with its northwest side closer to the observer.

NGC 1144 (a LIRG with $L_{\text{IR}} = 2.2 \times 10^{11} L_{\odot}$) has a Seyfert 2 spectrum (Osterbrock & Martel 1993), and radiates 35% of its $\lambda 10\mu\text{m}$ luminosity from a giant extra-nuclear star forming complex situated to the west of the active galactic nucleus (Joy & Ghigo 1988). Other morphological peculiarities are found in the radio (Condon et al. 1990). Aside from a weak radio emitting nucleus and emission from the Mid-IR star forming knots, extended non-thermal emission is seen along a prominent dust lane. Furthermore, the brightest radio emission in Arp 118 comes not from the nucleus, but from a double radio source observed 8 arcsecs to the northeast of the nucleus which straddles the dust lane. We will argue in Section 6, that these sources are physically located in Arp 118.

The peculiarities of NGC 1144 do not end with its dramatically different multi-wavelength appearance. Kinematically, NGC 1144 has long been known to rotate extremely rapidly (Hippelien 1989) showing a spread in velocity of over 1200 km s^{-1} across its disk (B99). Gao et al. (1997) mapped the ^{12}CO (1–0) emission in the galaxy, and confirmed that the galaxy’s molecular disk exhibits the same rapid rotation as the ionized gas. Their high resolution CO maps of NGC 1144 showed that the molecular gas is *not concentrated at the center of its disk*, but instead it is distributed asymmetrically around it—a very unusual situation for an violently interacting galaxy. The strongest concentrations were found in the south-eastern disk, the western star forming region and scattered clouds associated with the parts of the northern segment of the outer ring. The rapid rotation of the galaxy and the scattered ring was explained as being a consequence of a slightly-off center, but nearly head-on collision between NGC 1143 and NGC 1144 in the simulations of Lamb, Hearn & Gao (1998), leading to a spinning-up and partial expansion of the already massive target galaxy. The models were able to reproduce the basic morphology of the scattered ring, and one-armed spiral structure which dominates the disk of NGC 1144, though were less successful at modeling the velocity field.

Our previous low-resolution VLA study of the HI in Arp 118 (B99) was made with the C-array resulting in maps with a synthesized Gaussian beam with dimensions 21.2×17.0 arcsecs (HPBW). Faint HI ($M_{\text{HI}} = 7 \times 10^9 M_{\odot}$) emission was detected over a very narrow velocity range, and was concentrated towards the lowest observed velocities in NGC 1144. The HI seemed to anti-correlate with the brightest CO emission, both in velocity-space and spatially, although the spatial resolution was poor. The interpretation of the absence of HI over much of the velocity range of the CO emission was not straight forward. Faint HI absorption was seen in two narrow velocity bands within the velocity range in which CO (but not HI) emission was detected. This hinted at the possibility that, within the C-array beam,

HI emission might be masked by deep absorption over the same velocity range (roughly 800 km s^{-1}). Although this was a large range for HI absorption, HI profiles in other far-IR bright galaxies are known to be affected by absorption (see Mirabel & Sanders 1988). We predicted that if HI absorption had eaten away a large part of the “normal” disk HI profile, this would become obvious with higher resolution observations—allowing the absorption and emission to be easily separated spatially. This was the motivation for the new observations made with the B-array of the VLA.

We have organized the paper as follows: Section 2 describes the observations, Section 3 the HI observations, including the apparent HI/CO segregation and the HI absorption. In Sections 4 we discuss evidence for a large-scale shock-wave in the disk of NGC 1144. In Section 5 we discuss the possible origin of the HI/CO segregation, and present a gas-flow scenario that seems to explain many of the observed peculiarities of Arp 118. In Section 6 we explore the importance of the extremely luminous extra-nuclear radio sources which lie in the disk of NGC 1144. We present our conclusions in Section 7. Following B99, we will assume that $H_0 = 80 \text{ km s}^{-1} \text{ Mpc}^{-1}$ and a distance to Arp 118 of 110 Mpc.

2. Observations

The VLA observations¹ consisted of an 8 hr track made in B-array on June 23 1998, combined with a 4 hr track obtained previously in the C-array in 1996 (see B99). The new data were flux calibrated using 3C48. Phase calibration was performed by observing the nearby radio source 0320+052 (B1950) every 40 minutes during the observations. The calibrated B-array visibility data (uv data) were then merged with the calibrated uv data from the earlier observations to form a new dataset using the AIPS routine UVCOMB. The two separate IF band-passes were staggered such that two sets of 32 spectrometer channels overlapped, resulting in a velocity coverage of 2320 km s^{-1} (53 channels of width $193.5 \text{ kHz} = 43.8 \text{ km s}^{-1}$ in the rest frame of the galaxy) centered on $V_{\text{helio}} = 8721 \text{ km s}^{-1}$. The spectrometer settings were identical to those used in B99. The resulting channel maps had a synthesized HPBW of $6.2 \times 6.3 \text{ arcsecs}$. For some of the analysis we also created maps with a larger synthesized beam of $8 \times 8 \text{ arcsecs}$ and $15 \times 15 \text{ arcsecs}$, to improve our sensitivity to extended HI emission. We will mainly present the 8×8 maps here, resulting in ~ 2.5 times higher spatial resolution than the original B99 data. Continuum subtraction was performed following the method described in B99.

¹The National Radio Astronomy Observatory VLA is a facility of the National Science Foundation operated under cooperative agreement by Associated Universities, Inc.

As we shall show, HI emission and absorption was detected in a number of separated bands in velocity space, with large numbers of empty channels between these islands of emission. As such, the creation of an integrated HI map was more challenging than is usually the case when observing HI emission spread continuously throughout the data cube. Although the emission was easily seen in individual channels, the usual methods of blanking and performing the traditional “moment” analysis over the entire observed velocity range created a somewhat noisy result that did not match the quality of the individual channels in which emission was detected. As a result, we applied the “moment” analyses to groups of channels in which HI was detected, and the final result was summed to create the integrated HI emission map. Separate moment maps were created for those channels containing absorption and emission. Because the emission and absorption occurs in isolated regions of the data cube, we will not present iso-velocity and velocity dispersion maps. However, the kinematics of the gas is easily described in terms of the individual features in the cube.

3. The HI Properties and Kinematics

Figure 1 shows the integrated HI emission from the Arp 118 system superimposed on R-band images (from Hippelein 1989). Unlike our previous measurements based on C-array observation alone, the new observations resolve the HI clearly into emission regions which lie in the north-western half of the irregular ring of NGC 1144. We confirm (Section 4) that the HI absorption is weak, and restricted to the same narrow velocity ranges as reported in B99. A faint finger of emission also extends outside the ring in the direction of the elliptical companion NGC 1143. HI emission is absent to the levels of detection (3- σ upper limit is $0.85 \text{ mJy beam}^{-1} \text{ channel}^{-1}$) from at least half of the disk of NGC 1144, including the southern and eastern portions of the ring, the major star formation complexes in the south and western parts of the disk. The observations confirm that lack of emission, rather than emission eaten away by absorption, is responsible for the narrow HI line-width of NGC 1144.

Figure 2 shows the velocity field of the HI clouds derived from inspection of the individual channel maps. For context, the systemic velocities of NGC 1144 is $8648 \pm 14 \text{ km s}^{-1}$ and NGC 1143 is $8459 \pm 30 \text{ km s}^{-1}$ (Keel 1996)². We have labeled the emission clumps A through D for ease of identification.

²A number of different values for the velocity of NGC 1144 have been quoted in the literature. The 2-D H α velocity field presented in B99 based on Mt. Stromlo 2.3-m DBS spectroscopy shows that this velocity may not be representative of the *disk gas* at that position, but is characteristic of the velocity of the nucleus only. These discrepancies may indicate that highly non-circular motions present in the near-nuclear gas disk—a situation partly explained by our proposed model for the gas flows presented in this paper.

Region A' is the component of A that may be due to accreting gas onto the companion galaxy NGC 1143. Component A' has a narrow velocity width, and its mass is given in Table 1. The velocity of this feature is lower by almost 200 km s⁻¹ from that of NGC 1143, but it may be gas which has been pulled from the outer parts of NGC 1144 by the violence of the collision. On the other hand, we cannot rule out the possibility that it is disturbed gas in the outer regions of NGC 1144.

The clumpy emission at the north-western end of the outer ring (Region A) occupies the lowest velocity channels (8227–8270 km s⁻¹), and it is in agreement with the lowest velocities seen in the optical emission-lines in that region of the disk (B99). At higher velocities, a southern HI cloud complex B is seen at 8444–8531 km s⁻¹ tracking the rotation of the galaxy, as does region C to the north. These clouds have similar velocities to the relatively regular (but very rapid) rotation of the ionized gas disk of NGC 1144 mapped out in B99. One exception is emission region D, which has an extremely low velocity ($V=8183\text{ km s}^{-1}$), and is discrepant by approximately 900 km s⁻¹ compared with its expected velocity if it were to corotate with the inner ionized gas of NGC 1144 (No H α is observed in that direction). Since Region D is seen in two adjacent channels at the 3 and 3.5– σ level respectively, we presume it is real, despite its peculiar velocity. One explanation might be that the cloud is part of an extension of a faint optical loop seen to the far-east of NGC 1144 in the red continuum, and even more faintly in H α . Given the huge implied mass of NGC 1144 (as implied from the rapid rotation speed and the large velocity spread of 1200 km s⁻¹ seen in the ionized gas), this feature may be one of the few HI clouds seen in these observations which is not part of the peculiar disk of NGC 1144.

3.1. The “Yin-Yang”-like HI and CO Segregation in Arp 118

In Figure 3 we present the HI integrated map combined with the high resolution $^{12}\text{CO}(1-0)$ map of the molecular gas seen in Arp 118 by Gao et al. (1997). The new observations reveal an apparent separation between the CO and HI components, the CO emission being concentrated mainly in the south-eastern quadrant of the galaxy, and the HI in the north-western quadrant. Although there is some interleaving of the two components far from the center of NGC 1144, the HI and CO emission appears strongly segregated azimuthally with respect to the center—a highly unusual situation for a disk galaxy. It is this segregation that leads to the narrow line width in the HI line, since only part of the velocity field of the NGC 1144 is being represented in HI (see Figure 3 of B99 for a comparison with the CO profile).

In Figure 4 we present the integrated HI spectrum of the galaxy as derived from the

8×8 arcsecs (black histogram) and 15×15 arcsecs channel maps (grey histogram), as well as the spectrum obtained with the C-array only from B99 for comparison (open boxes). We do not recover all the flux seen in the large-beam C-array observations at the highest resolution (8×8 arcsec beam), but much more of the flux is seen in the intermediate-scale maps (15×15 arcsecs)—an indication that some of the gas is quite extended on the 15–20 arcsec scale. In Table 1 we present tabulated total masses of HI based on cubes made with small, intermediate and large beams. In general, we refer to B99 for a full discussion of the global properties of the galaxies. As the maps of B99 show, this emission extends over the NW half of the galaxy, and exhibits the same general anti-correlation with the CO as the more compact emission seen here (See Figure 5 of B99 for example). Our observations (maps not presented here for brevity) confirm the results of B99 for the extended gas. In this paper we will concentrate on the results of the observations with the highest resolution.

3.2. The HI Absorption Lines

Weak absorption features are seen in Figure 4, and they correspond closely in velocity to those seen with lower signal-to-noise in the C-array. Of interest is the absorption System 2, which appears slightly deeper in the current high-resolution observations than it did in the earlier (B99) low-resolution observations. The reason for this is also apparent in Figure 4. Faint emission, which is seen in the new observations to the north of the nucleus in the outer ring at $V = 8800 \text{ km s}^{-1}$ (the highest velocity feature in Figure 2) is observed at the *same velocity* as gas in the absorption system—these two features cancelled each other out in B99.

With the exception of this minor effect, the new results demonstrate that the absorption-line strength has not increased significantly compared with the previously published lower-resolution observations. In the earlier study we speculated that the absorption might be significantly larger than was observed (the “extreme absorber” hypothesis—see B99), if the absorption extended over the same velocity range as possible putative emission of similar strength within the large beam. However, the current observations do not reveal strong HI emission from the SE disk, nor is deep broad absorption detected. We can therefore rule out the peculiar shape of the HI profile as being a result of deep broad HI absorption.

In Figure 5 we present integrated maps of the HI absorption covering the velocity range of the two HI absorption features: System 1 at $8967\text{--}9099 \text{ km s}^{-1}$, and the slightly deeper System 2, at $8749\text{--}8880 \text{ km s}^{-1}$. The two systems are separated by $\sim 185 \text{ km s}^{-1}$, and do not share the same spatial centroid position. Instead they straddle the deep dust lane which crosses through the southern component of the bright double radio source (see Section 7), suggesting that the two components might be sampling the velocity jump across a very

powerful shock wave. We will return to this topic in Section 4.

The observed and derived properties of the absorption lines are given in Table 2. In addition to the kinematic properties of the absorption features (columns 2 and 3), we also present the average and maximum values of the 21cm line optical depth derived from the depth of the line at each channel. The results were derived from the 6.2×6.3 arcsec maps (see Section 2) to provide the highest discrimination of the background continuum. Care was taken to ensure that the continuum appropriate to the particular absorption system was used, since Systems 1 and 2 have different centroids. The derived HI column densities (Table 2: Column 6) assume the HI is uniformly distributed across a source having the same angular dimensions as the VLA beam, and as such represent strictly lower limits to the actual optical depths. More realistically in B99, despite the lower resolution, we estimated the optical depth by assuming that the HI absorption was seen against the compact double source, and used the fluxes for those sources on the arcsec scale from Condon et al. (1990). Using those assumptions, the column density was found in each line to be somewhat larger than in Table 2. Realistic values probably lie in between, and hence we conclude that the HI column densities in the two lines are in the range 5.5×10^{20} to 2×10^{21} atoms cm^{-2} .

In B99, we concluded that these column densities were consistent with 10–15 HI clouds of mass $M_{\text{HI}} \sim 8 \times 10^6 M_{\odot}$ within the VLA beam in order to avoid detecting the clouds in emission rather than absorption. These estimates are in good agreement with the new observations, if we make similar assumptions about the filling factors and continuum radio source sizes. Interestingly, the above HI column densities are high enough that it would be expected that the gas would be mainly molecular. The transition from mainly atomic to mainly molecular gas is believed to occur somewhere in the range of HI column densities between 4×10^{20} and 6.5×10^{20} at cm^{-2} ($3\text{--}5 M_{\odot} \text{ pc}^{-2}$) (Reach, Koo & Heiles 1994; Hidaka & Sofue 2002). Hence the HI absorption may be probing atmospheres of dense molecular condensations. Oddly, no bright CO emission is detected from the position of the bright radio source (see Figures 2 and 4). We will return to this point in Sections 6 & 7.

All things being equal, we can conclude from Table 2, that the HI column density for System 2 is almost twice that of System 1, a fact that is also consistent with the idea that the higher-velocity feature is sampling down-stream gas from the dust-lane/shock front (see Section 6).

4. Evidence for a Global Shock-wave in the Disk of NGC 1144

In this section we will present new evidence that suggests that NGC 1144 contains an unusually powerful global shock-wave coincident with a deep dust lane. The shock-wave may be an important clue as the mechanism for the apparent segregation of the HI and molecules in NGC 1144 (see Section 6)—inspiring the term “Yin-Yang” in the title of this paper.

Figure 6a shows an archival R-band (F606) continuum image of the inner portion of NGC 1144 obtained with WFPC2 on the Hubble Space Telescope (HST). The dominant features of the disk are a central bright bulge with fragmentary spiral arms, a massive star formation complex to the west of the nucleus (this is the same region which emits so much mid-IR luminosity Joy & Ghigo 1988), and a prominent dust lane (indicated by the arrows) which runs clockwise from a point southeast of the nucleus, towards the northwest. A further loop of star-clusters is also seen running from east to west along the southern extremities of NGC 1144, where it twists north to join the large western star-forming complex.

What is the nature of the dust-lane in NGC 1144 which seems so striking at optical wavelengths? Radio continuum observations may provide part of the answer. The optical morphology of the dust-lane is more easily traced in Figure 6b, which shows the same HST image after the application of an unsharp-mask. This helps to identify the high spatial-frequency components in the image, showing the strength and extent of the dust-lane, as well as allowing several shell-like features to be perceived to the west of the nucleus. We have also superimposed in this image the contours of the 20cm radio continuum of NGC 1144³. A close correspondence is seen between the position of the dust lane and the radio emission which seems to follow it all the way from its north-western tip down through the bright elongated source (this is resolved as a double by Condon et al. 1990), and through the twist of the dust-lane to the south and west. The southern component of the double source (see arrow in Figure 6b), lies suspiciously near the center ridge-line of the dust lane, providing further evidence that they might be causally related. Radio emission is also detected from the active nucleus and the western star forming complex.

The association of fainter radio emission with the dust-lane is strong evidence that the lane is a compression of the ISM. Similar radio continuum enhancements were detected in the ring galaxy VII Zw 466 (Appleton et al. 1999), and are common in shock waves associated with spiral arms (Rohde, Beck, & Elstner 1999; Wielebinski 2001). Cosmic ray particles radiate more efficiently when the magnetic field is compressed and magnetic field irregulari-

³The VLA radio continuum map of the A-array observations were kindly supplied by J. Condon (NRAO) and were presented in Condon et al. (1990).

ties are pushed closer together, trapping the cosmic rays for longer in the disk (see Bicay & Helou 1990; Appleton et al. 1999). Hence the radio observations support the idea that the dust-lane is a shock wave.

Further evidence that the dust-lane structure is purely hydrodynamic in nature rather than a traditional spiral density wave, is supported by the lack of association of an old stellar population with the dust-lane/filament. We show in Figure 7 the H α image of the galaxy superimposed with contours of the near-IR emission, as traced by the sum of its J, H, and K-band 2MASS images. The H α filament and dust lane have no counterpart in the near-infrared continuum light, strongly suggesting that the feature is a shock-wave in a purely gaseous disk with little detectable emission from an underlying stellar component.

Finally, there is kinematic evidence linking the dust lane to a powerful shock-wave. The HI absorption lines (Figures 4 and 5) show two velocity components separated by 185 km s $^{-1}$. Could the two components represent the up-stream and down-stream components of the gas entering and leaving the shock? Most normal streaming motions associated with spiral arms show quite modest velocity changes (10–20 km s $^{-1}$), so such a velocity jump across a shock would require unusual circumstances. The two components straddle the dust-lane, the higher velocity feature, System 1, is observed on the eastern side of the dust lane, whereas System 2 is to the west. Given the extremely rapid rotation of gas in NGC 1144 (circular velocities of at least 400 km s $^{-1}$) it would be relatively easy to deflect gas passing into the shock by an angle of \sim 30 degrees, in order to bring a substantial component of the rotational velocity into the radial line-of-sight direction—thereby increasing its line-of-sight velocity component. Further hints of this may be correct come from the kinematics of the CO clouds (clouds 9, 10 & 11 of Gao et al. (1997)) which show much higher velocities east of the dust lane than is observed along it. This is not unreasonable if the gas streams almost tangentially to the dust-lane after crossing the shock. If this is correct, then we would associate System 1 with neutral gas reforming down-stream of the shock, and System 2 with the upstream (unshocked) gas. In this case, the lower implied HI column of System 1 would result from this gas being depleted through ionization and/or molecular cloud formation (see Elmegreen 1993).

5. The Origin of the Apparent Segregation of Molecular/HI gas

The asymmetric azimuthal distribution and apparent segregation of HI and CO emission in NGC 1144 is very unusual when compared with both normal and violently collisional galaxies. Normal galaxies (whether barred or unbarred) generally have symmetrically disposed CO distributions with gas tending to centrate towards the center. For example, in a subset of the BIMA/SONG survey of nearby galaxies (e. g. Regan et al. 2001), only one

out of 15 galaxies showed strong asymmetries in the CO distributions—and even in that case (NGC 3627) the asymmetry was in the length of one spiral arm relative to another. None of these galaxies show the peculiar lop-sided CO distribution of NGC 1144. Massive CO clouds extending asymmetrically from the inner regions to the outermost extent of the disk are apparently very rare. Although HI asymmetries are more common in the outer parts of normal galaxies (see for example the recent study by Jog 2002), these are almost always associated with the faintest outer HI isophotes, the inner regions are usually less asymmetric.

However, even in interacting or merging systems, HI or CO asymmetries of the kind seen in NGC 1144 are surprisingly rare. If the two components are segregated, it is almost always radial segregation with strong CO emission at the center coincident with a nuclear starburst, HI in the outer parts in obvious tidal tails (e. g. Duc et al. 1997; Yun & Hibbard 2001). Even in the rare case where azimuthal asymmetry is seen in the outer HI component (e. g. Mk 273 or NGC 3921 Hibbard & Yun 1996; Hibbard & van Gorkom 1996), the HI is clearly part of a narrow, highly distinct tail, and not part of a coherent rotating disk, as in the case of NGC 1144.

Despite the differences between NGC 1144 and normal galaxies, studies of normal galaxies are not without relevance to this case. Molecular/HI phase transitions within normal disks have led to the concept of the “molecular front” pioneered by Sofue et al. (1995) and Honma et al. (1995), and based on the theoretical ideas of Elmegreen (1993). Here, an HI/H₂ phase-transition was used to explain why many galaxies are dominated by molecules in the center, but change suddenly to being HI-dominated further out. According to this picture, f_{mol} is critically dependant on the pressure confining the clouds P_e , the strength of the UV radiation field, and the metallicity of the gas. In normal galaxies, these parameters decline roughly exponentially with galactocentric radius, and provide a reasonable description of the sudden change from molecules to HI in a normal disk. In a collisional system like NGC 1144, the conditions in the galaxy are likely to be very different from the quiescent case. In particular, a non-axisymmetric one-armed shock could provide the necessary conditions for azimuthal CO/HI asymmetries.

In Arp 118, we have measured the value of $f_{mol} < 0.5$ in the bright HI regions to the west of the shock-wave, based on (3– σ) upper limits of $M_{H_2} < 5.7 \times 10^8 M_\odot$ from the CO observations of Gao et al. (1997)⁴ (after scaling to the HI beam), and is $> 96\%$ in the region of the bright molecular clouds, based on a similar HI upper limit of $M_{HI} < 1.1 \times 10^8 M_\odot$ from this paper. These results suggest that the CO and HI are not truly segregated, but

⁴The limit is based on the “standard” CO flux to H₂ mass conversion factor of $3 \times 10^{20} [\text{mol cm}^{-2}]/[\text{K km s}^{-1}]$.

that the molecular fraction changes dramatically across the shock-wave.

To demonstrate a possible causal relationship between the possible shock-wave and the CO/HI asymmetry, we show the distribution of CO and HI emission with the position of the shock-wave superimposed in Figure 8. The position of the shock is assumed to be coincident with the dust-lane/radio-continuum features of Figure 6. This demonstrates a number of interesting facts: 1) The majority (but not all) of the HI lies to the west of the dust-lane, 2) except at large galactocentric distances, all the centroids of the dense molecular cloud lie to the east of the dust-lane in the clouds associated with the northern half of the galaxy, and 3) HI absorption is seen *east* of the dust lane in a gap in the CO clouds. This gap (mentioned earlier) is centered on the 50 mJy radio source. The gap suggests that some local feed-back effects have disturbed the process of HI to H₂ conversion by rapidly turning H₂ into high mass stars and supernovae (Section 7). This supports the idea that the radio source is localized within Arp 118 and is not a powerful background object.

The strong shock would naturally explain why the disk of NGC 1144 is mainly molecular down-stream of the shock, and mainly HI upstream of the shock. Recently Hidaka & Sofue (2002) have extended the work of Sofue et al. (1995) to include spiral arm compressions, and found that HI would be transformed into H₂ on a timescale of < 5 Myrs upon entering a mild spiral perturbation. After undergoing compression, the molecular fraction reached almost unity (as in this case). After this initial transformation, the clouds slowly returned to a mainly HI form after about 25 Myrs, as a result of a reduction in the overpressure and an increase in the UV field due to star formation. The situation in NGC 1144 is different, because, if the work of Hidaka & Sofue (2002) is generally applicable to the very strong shock-wave we believe exists in NGC 1144, we have to explain why the molecular segregation extended over such a large area (almost half the galaxy) rather than a narrow region downstream of the compression.

Part of the explanation may come from the extremely rapid rotation of NGC 1144, combined with the peculiar streaming motions near the stronger-than-normal shock. In Figure 9 we show one plausible scenario for the apparent separation of the molecular and HI components on a galaxy-wide scale. Gas clouds, with molecular fractions more typical of the mid-radius molecular fraction (i.e. mainly HI-dominated ISM) rotate rapidly in a pre-collisional massive galaxy. The collision creates a quasi-stationary wave in the disk through which the HI clouds travel as they move from west to east (if the arm is trailing). The shock is strong enough to compress the clouds, causing them to become mainly molecular down-stream of the shock—as in the case of the galaxies discussed by Hidaka & Sofue (2002). However, unlike a normal disk galaxy, which may have circular velocities typically a 150-200 km s⁻¹, the clouds in NGC 1144 are travelling twice as fast.

Without a detailed model of the clouds entering the shock, we can only speculate about the likely streaming motions that might result—however the clouds are likely to be deflected inwards in a direction tangential to the shock—perhaps creating a flow of gas inwards towards, but overshooting the nucleus (see Figure 7). If as much as 30% of the rotational velocity was directed into such a flow, then the molecular material could travel around the galaxy and arrive roughly south of the nucleus in 30 million years—only a little longer than the timescale envisaged by Hidaka & Sofue (2002) for the molecular gas to remain in the dense phase in their picture. Overpressure effects from a pre-existing high-pressure starburst phase may also help to extend the timescale. Eventually, these clouds would disperse through the effects of star formation, returning unconsumed gas to a mainly HI-dominated phase shortly thereafter.

The advantage of this admittedly simple “sketch” of the gas flow in NGC 1144, is that it seems to account for a number of previously unexplained aspects of NGC 1144. Firstly, the inwardly directed stream might explain the odd fact that there are multiple velocity components in the H α velocity field in the vicinity of the nucleus (Hippelein 1989; Keel 1996), as well as large apparent gradients in the H α velocity field near the dust-lane (B99). A tangential flow along the dust-lane would also explain the strange optical loop observed in the HST image (Figure 6a) to the south and east of the nucleus, where the gas would swing in an anti-clockwise direction as it interacts with ambient lower-velocity gas in that regions. This interaction would explain why almost all of the star formation in NGC 1144 is concentrated either to the south and west of the nucleus in giant extended star formation complexes. Finally, the lack of CO emission in the center of NGC 1144 might also be a consequence of the fact that the molecular gas taking part in the flow would be less dissipative than diffuse gas, and would tend to overshoot the nucleus. Eventually, given enough time, this material may fall back to the center.

Figure 7 represents only one possible description of the complex phenomena that may be taking place in NGC 1144⁵. Our observations emphasize the need for gas-dynamical modeling that goes well beyond the usual single-phase models of the galaxy interactions. Indeed, the very high velocities, the unusually strong shock, and the likely multi-phase nature of clouds circulating within NGC 1144 provides a strong challenge to any hydrodynamic modeling effort.

⁵We note that if the spiral arm is leading rather than trailing (not consistent with other observation, nor published models), the gas flow through the shock would be reversed and the transition across the shock would be from molecules to diffuse HI.

6. The Nature of the Bright Double Radio Source in NGC 1144

What is the connection, if any, between the bright radio source and the dust-lane in NGC 1144? We indicated earlier that a luminous extra-nuclear radio source lies close to the ridge of the dust-lane. Although the radio contours show in Figure 6b (source indicated by an arrow) that the radio double appears blended into a single elongated source, it is easily seen as two sources in the original 1.49 GHz map of Condon et al. (1990), as well as in the 8.4 GHz VLA observations by Kukula et al. (1995). We also observe that the northern of the two sources is slightly elongated and less point-like in the higher resolution 6cm VLA observations. Its combined flux is 49 mJy at 20cm (about 1/3 of the total 20cm flux of Arp 118), which corresponds to a luminosity of $L_{20\text{cm}} = 7.08 \times 10^{22} \text{ W Hz}^{-1}$ if at the distance of NGC 1144⁶. To put this in perspective, it is similar to the *total* 20cm luminosity of M 82 and only ~ 3.7 times less than that of Arp 220 (Condon et al. 1990). Its steep spectral index (~ 0.9 see Jeske 1986) suggests a non-thermal origin.

Aside for the coincidence of the source lying in a “hole” in the CO distribution, the emission is unlikely to be a background galaxy on statistical grounds. According to J. Condon (NRAO – Private Communication) the probability of finding a 50 mJy source so close to the nucleus of NGC 1144 is about 1 part in 10,000 and consequently a spatial connection with Arp 118 is implied.

There are a number of possible explanations for the formation of a 50mJy radio source in the inner disk of NGC 1144. We can rule out radio supernovae (RSNe) for the radio emission. Firstly the spectrum of RSNe is much flatter (≤ 0.3) than measured values for the source (Jeske 1986). Our continuum observations (obtained as part of the data cube presented in this paper) recover the same flux for the double source as previously reported from observations obtained in 1987–88 (Jeske 1986; Condon et al. 1990). The fact that the source has not faded by a measurable amount over at least 14 years would contradict our current understanding of RSNe that they fade rapidly after reaching a peak of $L_{6\text{cm}} \sim 2 \times 10^{20} \text{ W Hz}^{-1}$ (see Chevalier 1982; Weiler et al. 1998). Furthermore, the luminosity of the double taken together is significantly brighter than the brightest known RSNe in M 82 or Arp 220. Since the peak 1.67 GHz radio power for the brightest RSN detected by Smith et al. (1998) in Arp 220 is $1.4 \times 10^{21} \text{ W Hz}^{-1}$, then one would need to have more than 45 *currently active* RSNe to account for the radio continuum flux. Such a scenario appears unlikely.

Another more likely explanation for the radio source is that it is due to prompt star

⁶We calculated the 1.49 GHz absolute spectral luminosity from $L_{20\text{cm}} = L_{1.49\text{GHz}} = 4\pi D^2 \times (1+z)^{(1+\alpha)} S$, where S is the 1.49 GHz flux density and $\alpha \sim 0.9$ (Condon et al. 1990).

formation from an unusually large compressed cloud which in turn generated multiple supernova explosions. The shock from the SNe could have destroyed/dissociated the molecules, apparently leaving the HI unaffected, and created a series of unresolved bubble-like emission regions similar to giant supernova remnants. The supernova rate needed to generate the observed radio flux can be calculated using the definition of Condon & Yin (1990)⁷ and is found to be $R_{SN}=0.78 \text{ yr}^{-1}$. This rate is surprisingly high for a region of just $\sim 1 \text{ kpc}$ in size, since it is ~ 7 times higher than the total supernovae rate of M82 (Huang et al. 1994), and similar to what is found in nuclei of ULIRGs. What is less clear is why this, and only this part of the shock-wave experienced such enhanced activity.

Based on numerical models, Lamb, Hearn & Gao (1998) speculated that the source marks the point of impact of the companion galaxy which collided 22 Myr ago. Star formation, created at that point by the increased density at the impact time, may have created many supernova which would provide the energy for the radio emission. One thing that is not clear in their models is why the impact site should lie so close to the current spiral shock. At the elapse-time in their simulation when the best match is made with the morphology of NGC 1144, the spiral-shock has already propagated well beyond the impact site and would no longer be in contact. Further observations will be required to gain more understanding of the nature of the radio-source and its environment.

7. Conclusions

We present high-resolution (VLA B & C array) HI observations of the Arp 118 (NGC 1144/3) system. Our main conclusions are:

- 1) The warmer neutral hydrogen gas and the cooler molecular gas is largely segregated azimuthally around NGC 1144 (leading to a Yin-Yang like-separation of the gaseous ISM). Most of the molecular gas is concentrated in the south-eastern half of the galaxy, and the HI in the north-west. The HI and molecular gas track the coherent, but very rapidly rotating, H α disk in NGC 1144. Because the two components appear segregated spatially, the gas is also kinematically segregated—the HI gas largely samples the low radial velocity end of the rotating disk, while the molecules sample the high-velocities. A complete picture of the rotation of the gas can only be seen when both components are considered together.

⁷The supernova rate can be estimated from the formula $L_{NT}(\text{W Hz}^{-1}) = 1.3 \times 10^{23} \left(\frac{\nu}{1 \text{ GHz}}\right)^{-\alpha} \left(\frac{R_{SN}}{1 \text{ yr}}\right)$, where $L_{NT} = L_{20\text{cm}} = 7.08 \times 10^{22} \text{ W Hz}^{-1}$ is the non-thermal radio luminosity, $\alpha=0.9$ is the radio spectral index, and R_{SN} is the rate of type II supernova (Condon & Yin 1990).

2) We suggest that the collision between NGC 1143 and NGC 1144 has initiated a phase transition in the ISM as outlined by Elmegreen (1993). HI and CO clouds are seen along an interface region which coincides with a dark, extremely sharp, dust-lane seen on an HST image of the galaxy. Combined with other evidence, we suggest that the dust-lane is a collisionally induced shock-wave that may be responsible for the conversion of diffuse HI clouds (molecular fraction < 0.50) into dense molecular-dominated (molecular fraction > 0.96) cloud complexes as they pass through the shock-wave. Because of the extremely rapid rotational velocities in the galaxy (the overall velocity spread is 1200 km s^{-1}), the gas can orbit a significant distance around the galaxy after the compression before the residual molecular clouds (not consumed in the associated star formation) are converted back to HI again-leading to an apparent large-scale segregation.

3) Further evidence of a strong shock within the disk of NGC 1144 comes from the discovery of two HI absorption-lines, separated by 185 km s^{-1} , which are seen against the brightest radio source which lies close to the center-line of the dust lane. The HI absorption lines lie on either side of the dust-lane, and may be sampling gas clouds entering the shock, and reforming with much lower column-density further down-stream. If this explanation is correct, then the velocity-jump implies large streaming motions almost parallel to the dust-feature which would funnel gas inwards to overshoot the nucleus. This is consistent with both the loopy morphology of NGC 1144 in this region, and the unusually large non-nuclear star formation in the disk. This high angular-momentum gas stream may explain the lack of molecular pile-up in the center of the galaxy—a situation that is unusual for a violently collisional system with this level of far-IR luminosity ($L_{\text{IR}} = 2.2 \times 10^{11} L_{\odot}$) .

4) Although faint (2–3 mJy) radio emission is seen associated with the dust-lane, symptomatic of mild magnetic field compression, the double radio source mentioned above may be a hot-spot $20\text{--}30\times$ more powerful than the rest of the dust-lane. Although we cannot completely rule out the possibility that the source is a distant background object, the positional agreement with the dust-lane center suggests that it is associated with NGC 1144. We speculate that the source represents emission from cosmic rays released by an episode of massive star formation and supernova explosions. A gap is also seen in the molecular cloud distribution coincident with the radio source position, suggesting that the process that created the source has either disrupted the transformation of HI into H₂ in that region, or has rapidly turned the H₂ into massive stars. Further observations, especially in the near and mid-IR will be needed to understand the processes which have given rise to the bright radio source region.

5) HI emission is observed extending beyond the outer disk of NG 1144 towards the elliptical companion NGC 1143. This gas may represent the early stages of matter transfer

between the two galaxies. The gas mass involved is small ($M_{\text{HI}} = 2 \times 10^8 M_{\odot}$) but provides further evidence that the two galaxies have recently collided.

PNA wishes to thank W. Reach (SSC-Caltech) for interesting discussions, and James Condon (NRAO) for the radio continuum image of Arp 118 and discussions relating to the eastern radio double source. VC would like to acknowledge the partial support of JPL contract 960803. This research has made use of the NASA/IPAC Extragalactic Database (NED) which is operated by the Jet Propulsion Laboratory, California Institute of Technology, under contract with the National Aeronautics and Space Administration. Based on observations made with the NASA/ESA Hubble Space Telescope, obtained from data archive at the Space Telescope Science Institute. STScI is operated by the Association of Universities for Research in Astronomy, Inc. under the NASA contract NAS 5-26555.

REFERENCES

Appleton, P. N., Charmandaris, V., Horellou, C., Ghigo, F., Higdon, J., & Lord, S. 1999, ApJ, 527, 143

Appleton, P. N., Charmandaris, V., Gao, Y., Combes, F., Ghigo, F., Horellou, C., & Mirabel, I. F. 2002, ApJ, 566, 682

Barnes, J. E., & Hernquist, L. 1996, ApJ, 471, 115

Bekki, K., & Noguchi, M. 1994, A&A, 290, 7

Bicay, M., & Helou, G. 1990, ApJ, 362, 59

Braine, J., Duc, P.-A., Lisenfeld, U., Charmandaris, V., Vallejo, O., Leon, S., & Brinks, E. 2001, A&A, 378, 51

Bransford, M. A., Appleton, P. N., McCain, C. F., & Freeman, K. C. 1999, ApJ, 525, 153 (B99)

Bryant, P. M., & Scoville, N. Z. 1999, ApJ, 117, 2632

Casoli, F., Willaime, M.-C., Viallefond, F., & Gerin, M. 1999, A&A, 346, 663

Chen, J., Lo, K. Y., Gruendl, R. A., Peng, M.-L., & Gao, Y. 2002, AJ, 123, 720

Chevalier, R. A. 1982, ApJ, 259, 302

Condon, J. J., Helou, G., Sanders, D. B., & Soifer, B. T. 1990, *ApJS*, 73, 359

Condon, J.J., & Yin, Q.F. 1990, *ApJ*, 357, 97

Downes, D., & Solomon, P. M., 1998, *ApJ*, 507, 615

Duc, P.-A., Brinks, E., Wink, J. E., & Mirabel, I. F. 1997, *A&A*, 326, 537

Dinh-V-Trung, Lo, K.Y., Kim, D.-C., Gao, Y., & Gruendl, R.A. 2001, *ApJ*, 556, 141

Elmegreen, B. G. 1993, *ApJ*, 411, 170

A.S. Evans, Mazzarella, J.M., Surace, J.A., & Sanders, D.B. 2002, *ApJ*, (In Press–astro-ph/0208541)

Freeman, K., & de Vaucouleurs, G. 1974, *ApJ*, 194, 569

Gao, Y., Solomon, P. M., Downes, D., & Radford, S. J. E. 1997, *ApJ*, 481, L35

Gao, Y. & Solomon, P. M. 1999, *ApJ*, 512, L99

Georgakakis, A., Forbes, D. A., & Norris, R. P. 2000, *MNRAS*, 318, 124

Hibbard, J. E., Guhathakurta, P., van Gorkom, J. H., & Schweizer, F. 1994, *AJ*, 107, 67

Hibbard, J. E., & van Gorkom, J. H. 1996, *AJ*, 111, 655

Hibbard, J. E., & Yun, M. S. 1996, in *Cold Gas at High Redshift*, eds. M. Bremer, H. Rottgering, P. van der Werf, & C. L. Carilli (Dordrecht: Kluwer), p47

Hidaka, M., & Sofue, Y. 2002, *PASJ*, 54, 223

Hippelein, H. H. 1989, *A&A*, 216, 11

Hollenbach, D., & McKee, C. 1989, *ApJ*, 342, 306

Honma, M., Sofue, Y., & Arimoto, N. 1995, *A&A*, 296, 33

Huang, Z. P., Thuan, T. X., Chevalier, R. A., Condon, J. J., & Yin, Q. F. 1994, *ApJ*, 424, 114

Jeske, N. A. 1986, Ph.D. thesis, University of California, Berkeley

Jog, C. J. & Solomon, P. M., 1992, *ApJ*, 387, 152

Jog, C. J. 2002, *A&A*, 391, 471

Joy, M., & Ghigo, F. 1988, *ApJ*, 332, 179

Keel, W. C. 1996, *AJ*, 111, 696

Kukula, M. J., Pedlar, A. Baum, S. A., & O'Dea, C. P. 1995, *MNRAS*, 276, 1262

Lamb, S. A., Hearn, N. C., & Gao, Y., 1998, *ApJ*, 499, L153

Lo, K. Y., Gao, Y. & Gruendl, R. A. 1997, *ApJ*, 475, L103

Mihos, J. C., & Hernquist, L. 1996, *ApJ*, 464, 641

Mihos, J. C. *ApJ*, 550, 94

Mirabel, I. F., & Sanders, D. B. 1988, *ApJ*, 335, 104

Noguchi, M. 1988, *A&A*, 203, 259

Osterbrock, D E., & Martel, A. 1993, *ApJ*, 404, 551

Regan, M. W., Thornley, M. D., Helfer, T. T., Sheth, K., Wong, T., Vogel, S. N., Blitz, L. & Bock, D. C.-J. 2001, *ApJ*, 561, 218

Reach, W. T., Koo, B-C. & Heiles, C. 1994, *ApJ*, 429, 672

Rohde, R., Beck, R. & Elstner, D. 1999, *A&A*, 350, 423

Sanders, D. B., & Mirabel, I. F. 1985, *ApJ*, 298, L31

Sanders D. B. & Mirabel, I. F. 1996, *ARA&A*, 34, 749

Sargent, A. I., & Scoville, N. 1991, *ApJ*, 366, 1

Scoville, N. Z., Sanders, D. B, Sargent, A. I., Soifer, B. T., & Tinney, C. G. 1989, *ApJ*, 345, L25

Scoville, N. Z., Sargent, A. I., Sanders, D. B., & Soifer, B. T. 1991, *ApJ*, 366, L5

Smith, H. E., Lonsdale, C. J., Lonsdale, C. J., & Diamond, P. J. 1998, *ApJ*, 493, L17

Sofue, Y., Honma, M., & Arimoto, N. 1995, *A&A*, 296, 33

Wang, W-H., Lo, K. Y., Gao, Y. & Gruendl, R. A. 2001, *AJ*, 122, 140

Weiler, K. W., van Dyk, S. D., Montes, M. J., Panagioptoi, N., Sramek, R. A. 1998, *ApJ*, 500, 51

Wielebinski, R. 2001, in ASP Conf. Ser. 230, Galaxy Disks and Disk Galaxies, ed. J. G. Funes & E. M. Corsini (San Francisco: ASP), 165

Yun, M. S., & Hibbard, J. E. 2001, ApJ, 550, 104

Table 1. Properties of the Galaxies

Name	Type	D (Mpc)	V_{helio}^a (km s $^{-1}$)	ΔV_{HI} (km s $^{-1}$)	ΔV_{CO+HI}^b (km s $^{-1}$)	M_{HI}/M_{\odot}^c ($\times 10^9$)	M_{HI}/M_{\odot}^d ($\times 10^9$)	M_{HI}/M_{\odot}^e ($\times 10^9$)
NGC 1144	S _{pec} -Ring	110	8648 \pm 14	170 ^b	1120	2.0	5.6	7.0
NGC 1143	E/S0 _{pec}	110	8459 \pm 30	44 ^f	–	0.2 ^f	–	–

^aThe optical velocities are from Keel (1996).

^bfrom our earlier paper (B99).

^cHI masses from the brighter features from this paper based on 8 \times 8 arcsecs restored beam (see text).

^dHI masses from this paper based on 15 \times 15 arcsecs beam (see text). Note that considerably more extended emission is detected.

^eHI properties from low-resolution 21.2 \times 17.0 arcsecs beam presented in B99 using C-array only.

^fAssuming extension at $V = 8270$ km s $^{-1}$ within optical envelope is associated with NGC 1143 (see text).

Table 2. Properties of Absorption-Line Systems

System	V_{helio} (km s^{-1})	ΔV_{FWHM} (km s^{-1})	$\langle \tau \rangle^a$	τ_{max}	N_{HI} $\times 10^{20} \text{ atoms cm}^{-2}$
System I	9050 ± 20	100 ± 30	0.023	0.027	$5.5 \times T_{s100}$
System II	8825 ± 21	140 ± 30	0.036	0.044	$11.5 \times T_{s100}$

^aOptical depths calculated using background continuum map derived from this data—not shown, and assuming the radio source fills the 6.2×6.3 arcsec beam (this is therefore a strict lower limit—see text). The average optical depths shown are the average optical depths over the channels in which absorption was detected. Note T_{s100} = an assumed spin temperature in units of 100 K.

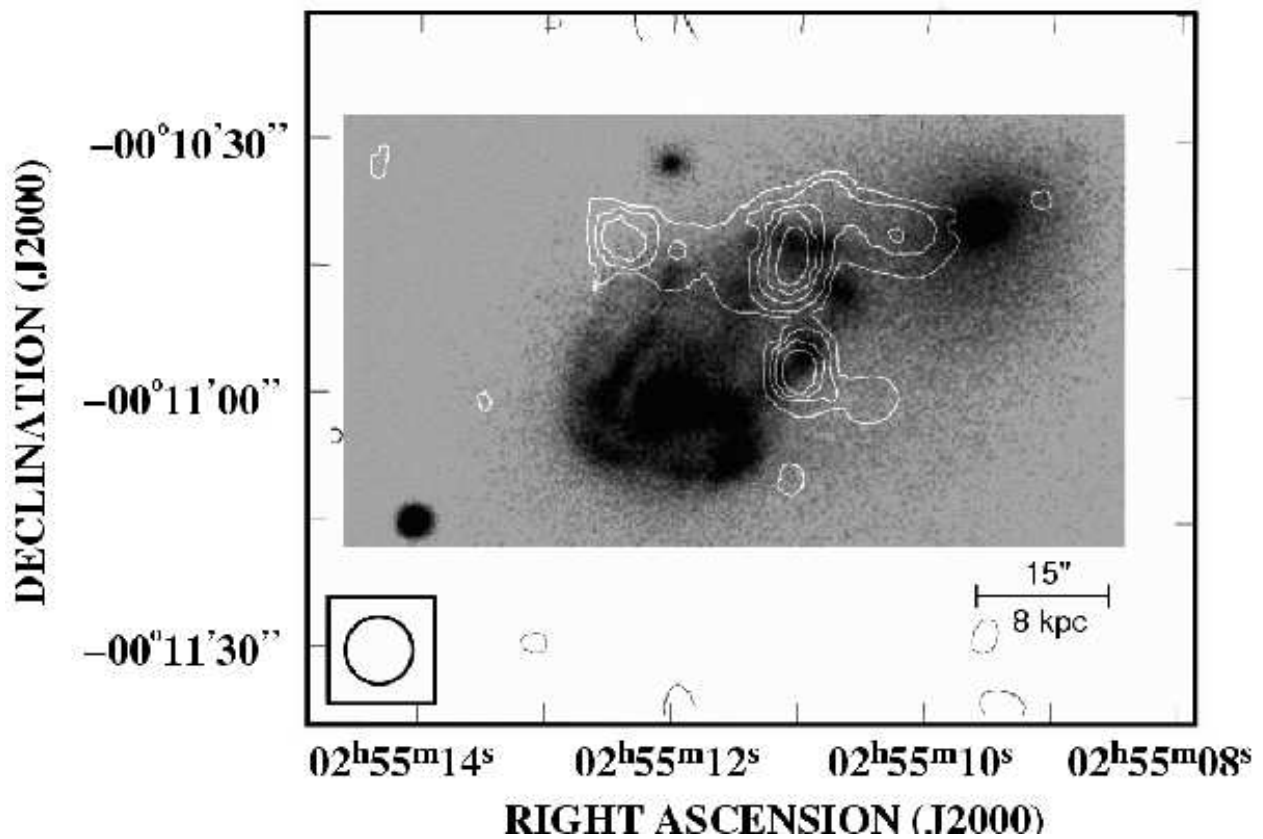


Fig. 1.— The integrated HI surface density map superimposed on an r-band plate of Arp 118 from Hippelein (1989). The ring galaxy NGC 1144 is to the south-east, and E2/S0 galaxy NGC 1143 to the north-west. Contour levels are 1, 2, 3, 4, 5, 10, 15 \times 33.9 mJy beam $^{-1}$ km s $^{-1}$ or units of 5.8×10^{20} atoms cm $^{-2}$.

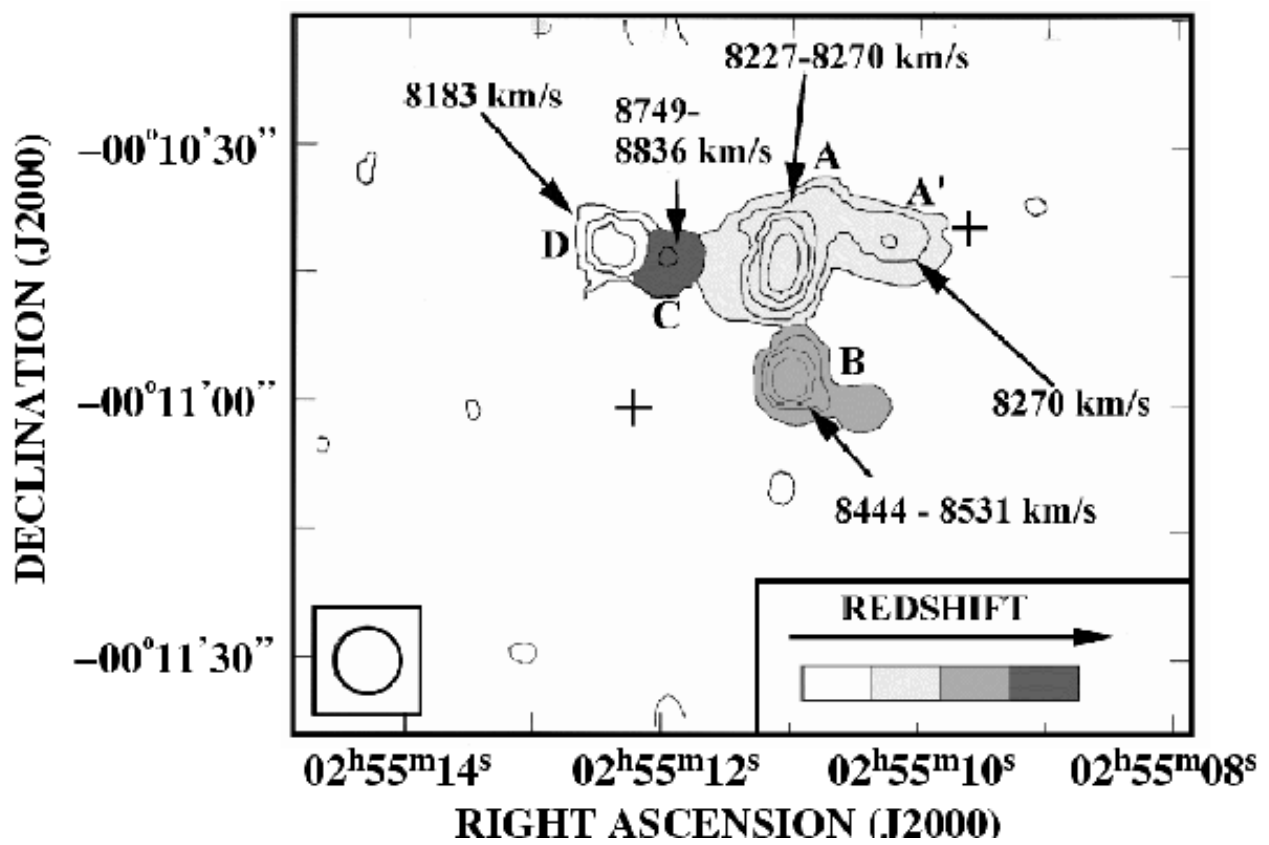


Fig. 2.— The heliocentric radial velocities of the HI emission regions (km s^{-1}). The crosses mark the centers of NGC 1144 and NGC 1143.

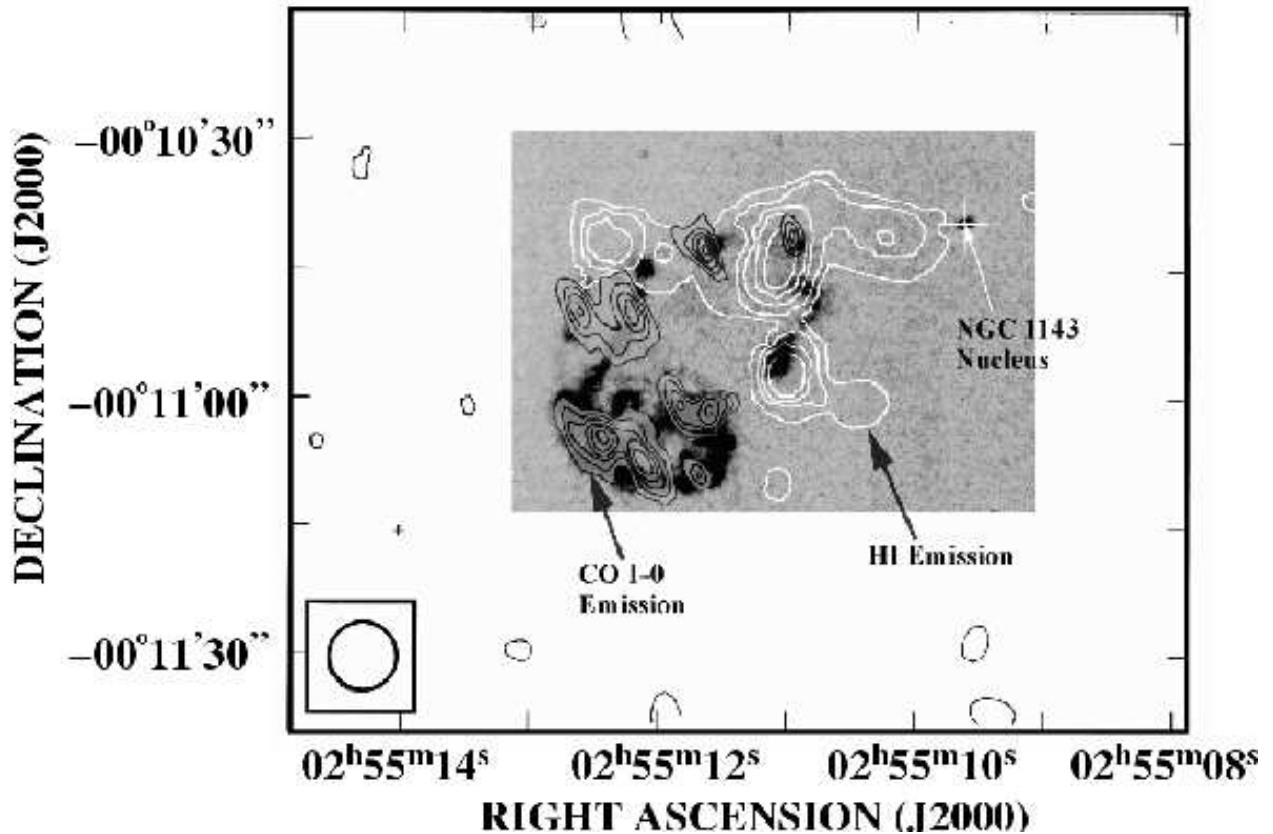


Fig. 3.— The combined molecular and neutral gas content of Arp 118 superimposed on the greyscale image of $\text{H}\alpha$ emission from Hippelein (1989). The $^{12}\text{CO}(1-0)$ emission contours from Gao et al. (1997) are shown in grey starting at $5.14 \text{ Jy km s}^{-1} \text{ beam}^{-1}$ and increasing by $3.86 \text{ Jy km s}^{-1} \text{ beam}^{-1}$. The HI contours of Figure 1 are also included in white (for units see Figure 1). Note the remarkable segregation of the neutral and molecular gas.

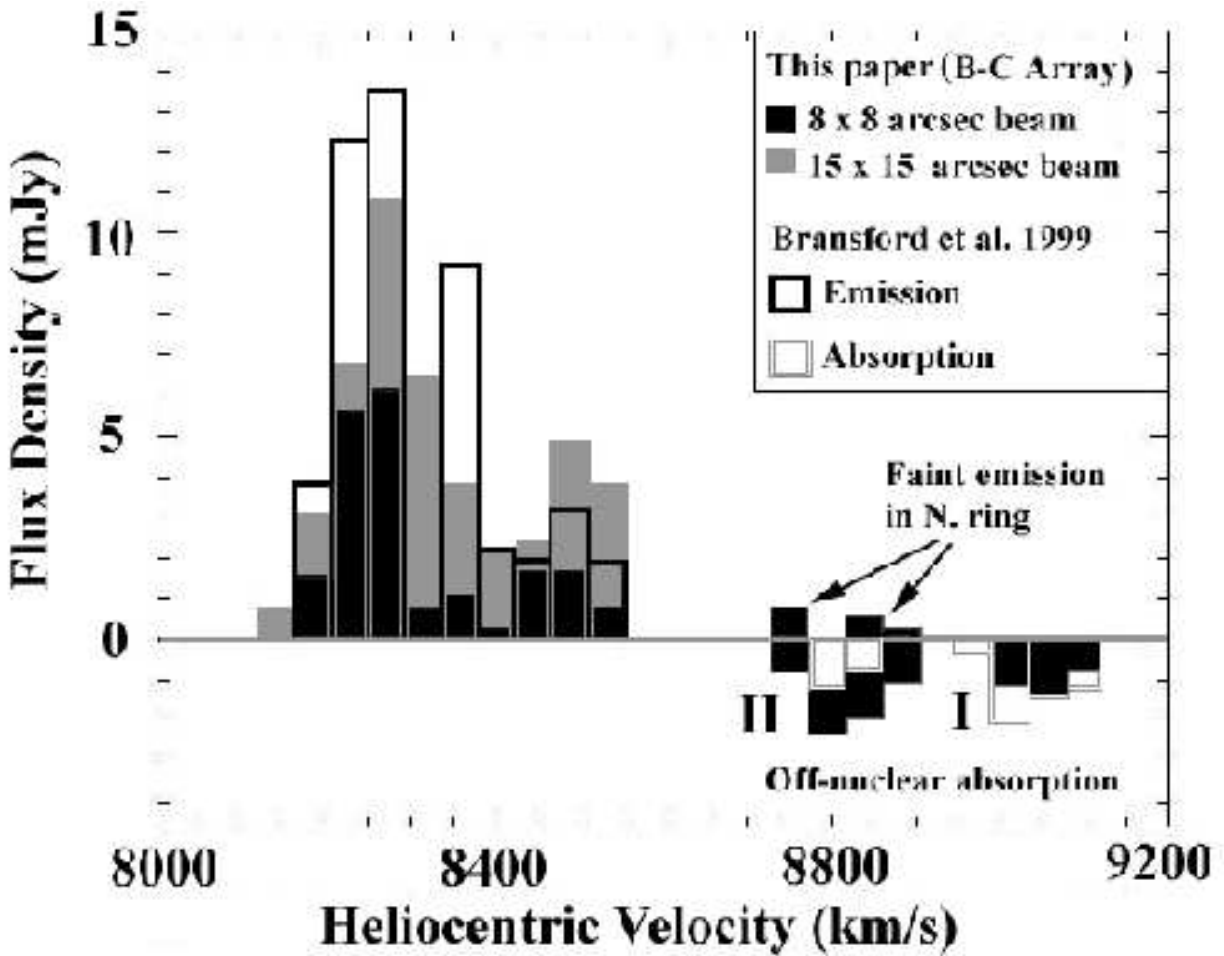


Fig. 4.— The integrated HI spectrum derived from the new combined B-C Array data and our original lower-resolution C-array observations (see key for color coding). Newly detected weak emission near $V = 8800 \text{ km s}^{-1}$ from the northern ring was absent from the older observations because it was nullified by the faint absorption seen near the center of the galaxy. Despite this, the new observations confirm the earlier result that the HI emission occupies a much smaller range of radial velocities than seen in the ionized gas disk because of spatial segregation.

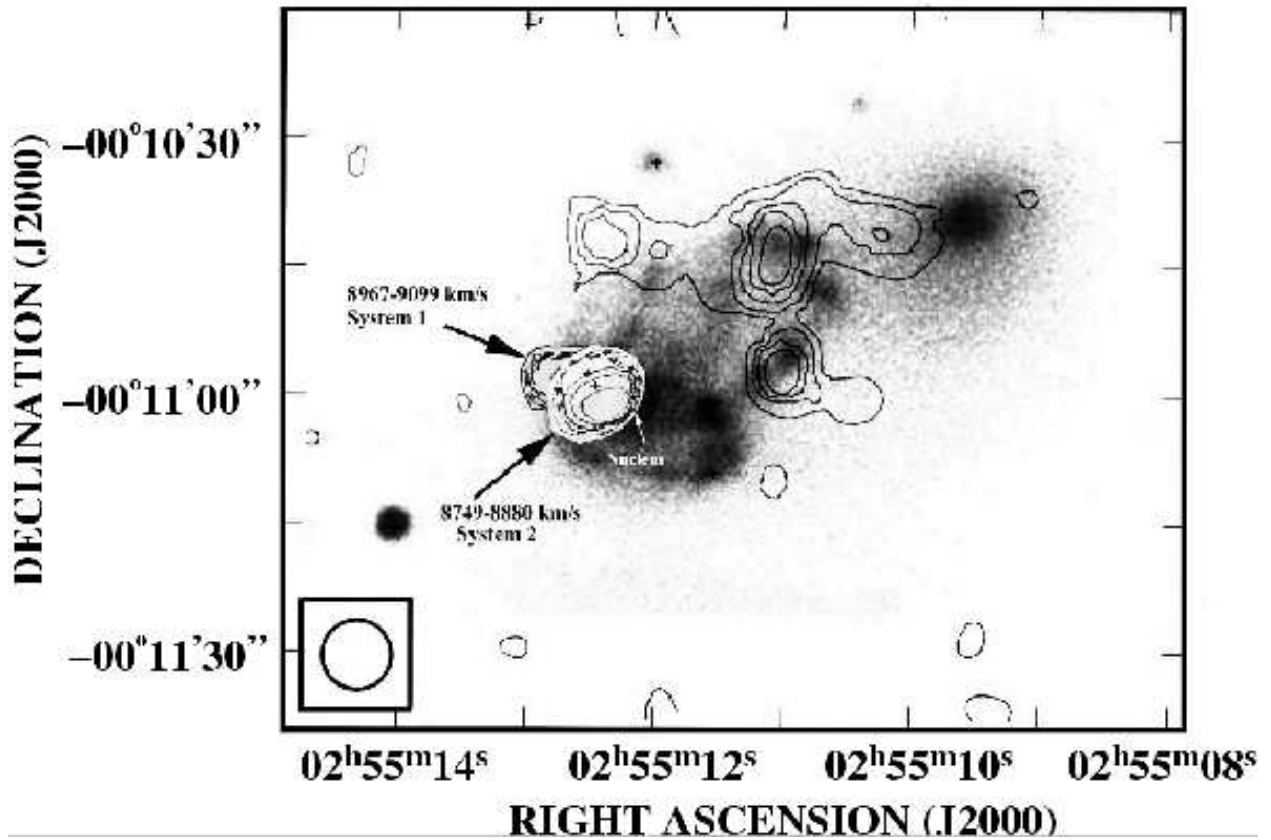


Fig. 5.— The HI absorption (System 1 and 2) seen superimposed on the R-band image of Arp 118. Note that the absorption is seen against the 50 mJy double radio source (dark crosses denote centroid of double source) discovered by Condon et al. (1990) which lies just to the east of the nucleus. The fainter nucleus of NGC 1144 does not show HI absorption (white cross). Absorption contour units are -3 , -2.7 , -2.3 , -1.9 , -1.5 mJy beam $^{-1}$. Emission lines contours in black—units see Figure 1.

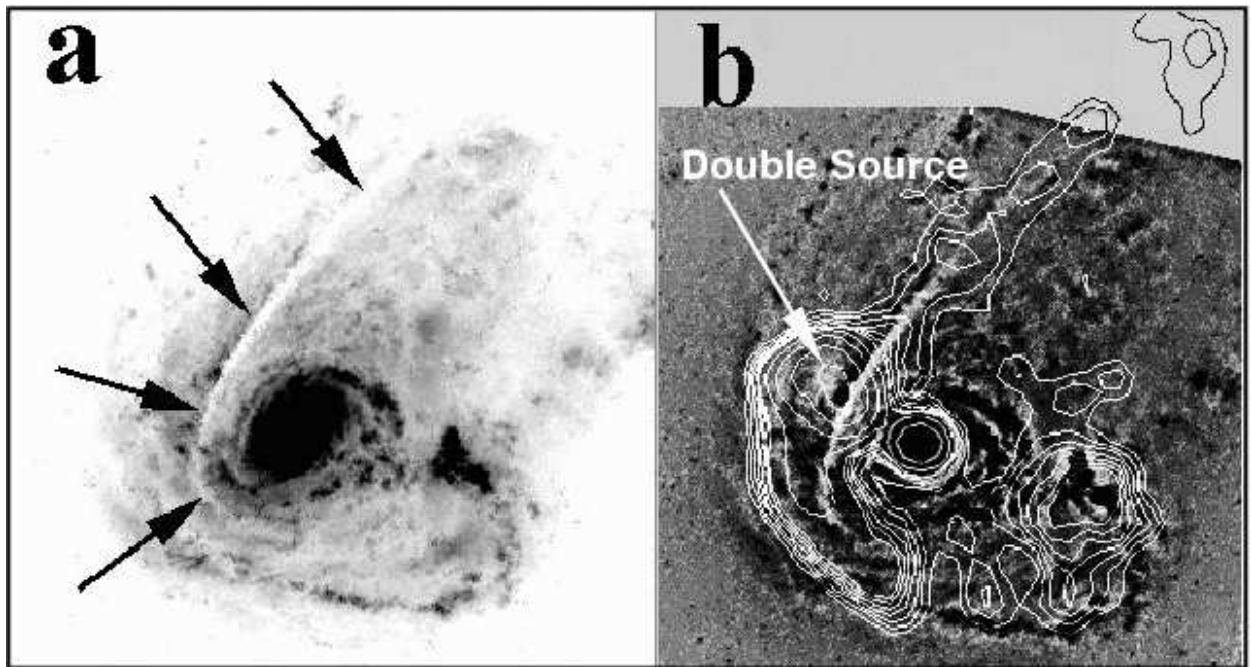


Fig. 6.— The F606 red continuum image from WFPC2: (a)(grayscale) showing the dominant morphological features of NGC 1144. Note the prominent dust lane (arrows) which is seen more clearly in (b), where the image (grayscale) has been unsharp masked to reveal the small-scale structure in the image. Contours show 20cm VLA radio continuum emission from Condon et al. (1990), and seems to follow the dust lane very closely over most of its length.

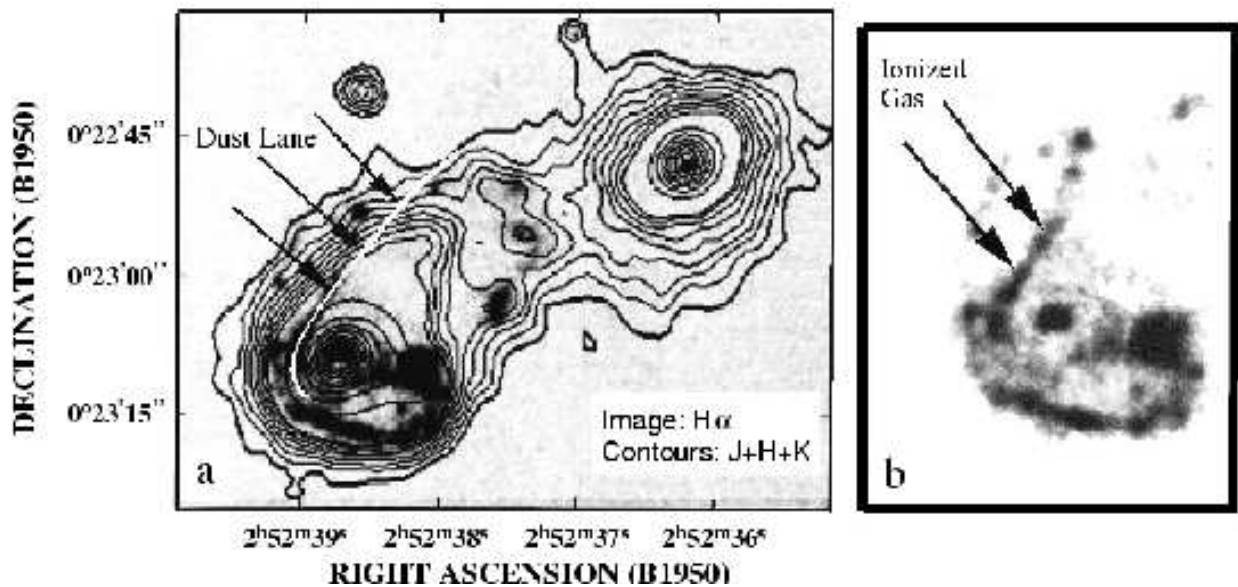


Fig. 7.— (a) The sum of J, H and K-band images of Arp 118 from 2MASS (contours) superimposed on the H α +N[II] image (grayscale). The dust lane is also marked as a white line. (b) For clarity, the inner part of NGC 1144 is shown again in H α +N[II] light without the dust lane position. The bright ionized gas filament marked with the arrow is almost coincident with the inner segment of the dust-lane. Note that the dust-lane/H α filament shows a complete mis-match with the near-IR light, implying that the feature is a transient hydrodynamic structure rather than a density wave with an underlying old stellar population.

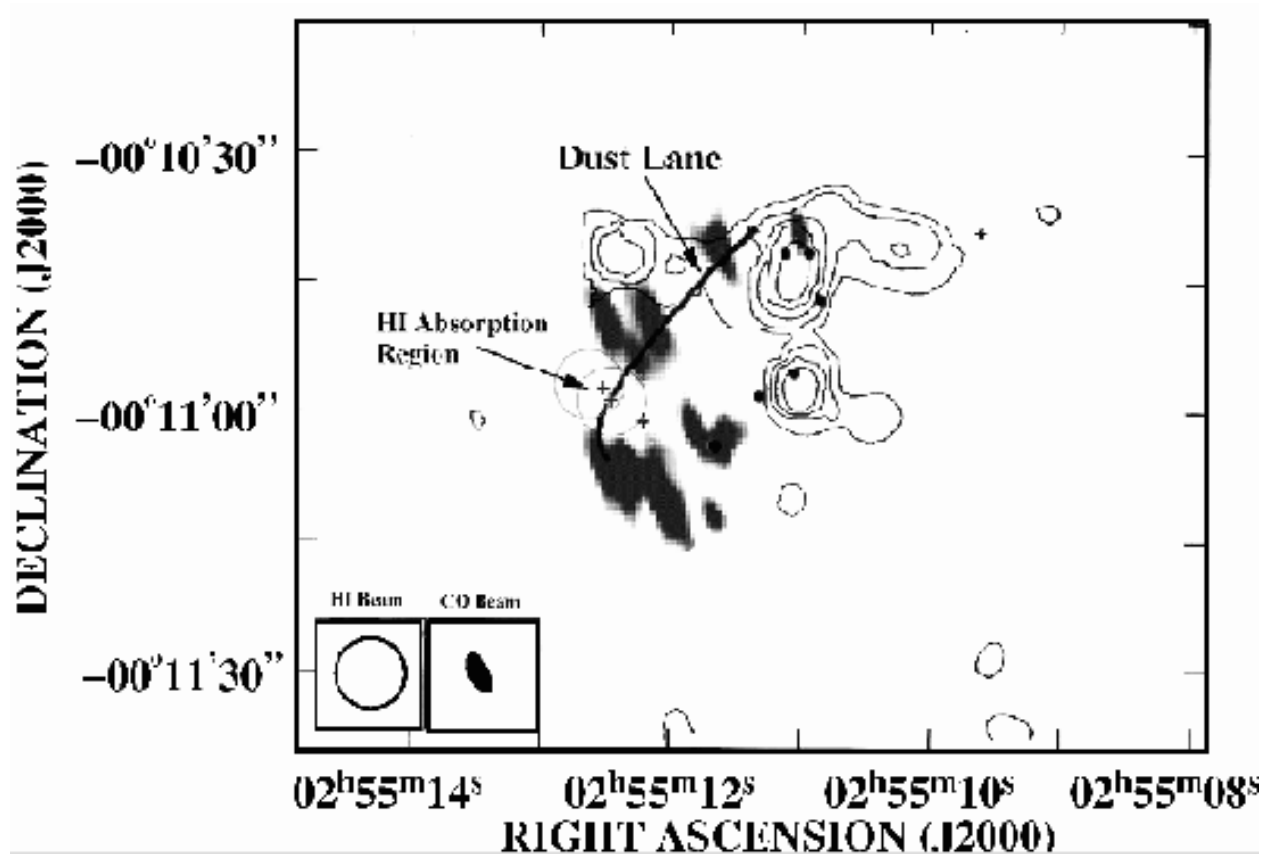


Fig. 8.— The locus of the center of dust lane marked onto a plot of the HI and CO distributions in Arp 118. The dust lane's position was traced a little beyond the HST WFPC2 image of Figure 5, by assuming that it is traced by the radio continuum ridge. The three crosses mark the positions of the double radio source (close to the dust lane), and the nucleus to the south and west.

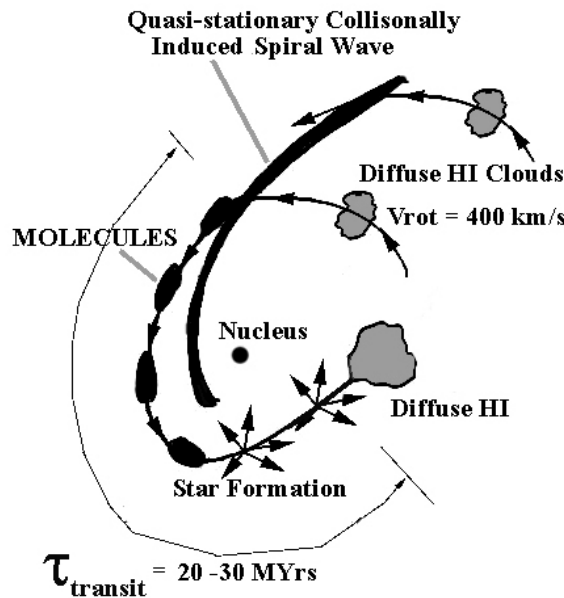


Fig. 9.— A schematic representation of how HI and molecules may be segregated in NGC 1144. HI clouds, circulating in a counter-clockwise manner in the rotating disk of NGC 1144, encounter the strong shock wave are compressed becoming mainly molecular (Elmegreen 1993). The clouds are deflected by the shock inwards. Eventually, star formation destroys the molecules and they circulate rapidly to the west, becoming mainly neutral hydrogen-dominated again. The unusually rapid rotation of NGC 1144, combined with the transient one-armed spiral shock-wave leads to the appearance of large-scale segregation of the HI and molecules.